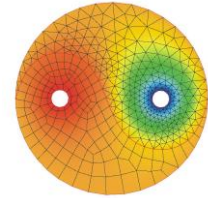




Publishing House
AKAPIT



SEDIMENTATION IN BINARY Cu-Sn SYSTEM

DARIA SERAFIN, WOJCIECH J. NOWAK, BARTEK WIERZBA*

*Rzeszow University of Technology, Faculty of Mechanical Engineering and Aeronautics,
al. Powstańców Warszawy 12, 35-959 Rzeszow, Poland*

**Corresponding author: bwierzba@prz.edu.pl*

Abstract

In the present paper the sedimentation process in binary multiphase Cu-Sn system is presented. The initial samples were produced by GoodFellow, the initial molar fraction was Cu₃₀Sn₇₀ respectively. Thus, the two-phase region was obtained. The two different phenomena occurs during the process of sedimentation at 453K for 1 hour with the angular speed of 35 000 RPM . Mainly, the Cu₃Sn and Cu₆Sn₅ phase growth due to the temperature and migration of pure Sn according to the centrifugal force. Both phenomena's are described by physical equations. The model describing the phase growth based on the Leibnitz rule - the mass conservation law at the moving boundary and the migration of the elements due to the sedimentation is characterized by equation of motion. The results of the presented models are shown.

Key words: Sedimentation, Diffusion, Mathematical modelling

1. INTRODUCTION

Sedimentation is widely known term describing the transport phenomenon of macroscopic particles, which may be induced by gravitational or centrifugal forces (Mashimo, 1988). Initially this term was mostly connected with liquid solvents and macromolecules. Driving force for the sedimentation process had been defined by Lamm as a difference between centrifugal force and the buoyant force produced by liquid solvent (Demeler & Saber, 1998). Lamm's Laws initiated mathematical approach to solid – liquid systems' behaviour under external force field (Lamm, 1929). Increasing interest in sedimentation processes in biochemistry resulted in invention of ultracentrifuge machines, which performances, mostly maximum rotation rates and inner diameters improved over the years (Mashimo et al., 1996). Development in experimental abilities caused new applications of ultracentrifuge machines, e.g. in sedimentation process in condensed matter. Such attempts had been performed for the first time by Barr and Smith (1969) and by Anthony (1970) and concerned sedimentation of gold atoms in pure metals

characterized by low melting point: potassium, indium and lead. Observations and analysis of sedimentation effects in solid states required, however, further developments in machinery – it resulted in construction of new ultracentrifuge apparatus, developed by Mashimo et al. (1996). New machine enabled to generate an acceleration field up to 106 g at high temperatures and for a long time. Those characteristics are essential in sedimentation in solid state, for instance, combination of them can induce segregation (Mashimo et. al, 2008) or separation of isotopes (Ono et al., 2009) and both structural changes and evolution of atomic scale graded structure in condensed matter due to migration of atoms and voids (Huang et al., 2004).

Such numerous effects that are observed in solids under centrifugal field present the great potential of sedimentation process – it enables for production of new, high quality materials but also helps to control e.g. lattice order or chemical concentration of alloy components and, therefore, to control or improve the properties of a material (Wierzba & Nowak, 2018). Moreover, the ability of mathematical description of atomic phenomena helps to predict

the micro and macro- effects observed in the metal under certain conditions of temperature, time and external force field (Wierzba, 2017).

Thus, in the present paper, the experimental results of sedimentation process of binary multi-phase Cu₃₀Sn₇₀ at 453K with the rotation rate of 35 000 RPM are presented. The sedimentation in Cu-Sn system has been already investigated by Wierzba et al. (2018), however, in this work different initial composition of the alloy and different experimental conditions have been adopted. Moreover, the two-phase region observed in Cu₃₀Sn₇₀ enables implementing a new model, based on the Leibnitz rule, describing the phase growth and morphology changes during the testing in ultracentrifuge apparatus. Such model may be potential method for predicting the alloy's behaviour at the given conditions. The verification of model applicability was performed by comparison of experimental and analytical results.

2. EXPERIMENTAL

Samples of binary Cu-Sn alloy had been prepared with nominal composition 30%Cu, 70%Sn (in at. %) by machining rods out of cast alloy. The diameter of the rods were 2 mm and their length 5 mm. Some additional physical parameters of Cu and Sn that are important in sedimentation process are shown in table 1. Samples were then fixed in titanium holder of ultracentrifugal Schenck apparatus. The distance between the holder and the centre of rotation was 88 mm. The testing was performed at 453 K for 1 hour with angular speed of 35 000 RPM. After centrifugation, tested samples and samples in as-cast condition were mounted using CitoPress-5 equipment in the thermosetting resin PolyFast (both produced by Struers). To reveal microstructure of the samples, metallographic cross sections were prepared in grinding and polishing processes. Final polishing was conducted using woven cloth and SiO₂ suspension with 0.25 μm granulation. Such cross-sections were tested in term of their chemical composition using scanning electron microscope Hitachi S3400N. The microstructure observations were conducted using both scanning electron microscope Hitachi S3400N and Nikon Epiphot 300 light

microscope. The former is equipped with camera and NIS Elements software for digital image analysis, which enabled to measure fraction of particular phases. Three different measurements were performed for each sample and the average value and standard deviation were calculated.

Table 1. Parameters of Cu and Sn (Haynes, 2009).

Component	Molar mass, g/mol	Molar volume at 500 K, cm ³ /mol	Density at 500 K, g/cm ³	Initial composition, at. %
Cu	63.546	7.164	8.87	30
Sn	118.71	16.510	7.19	70

3. EXPERIMENTAL RESULTS

The SEM analysis of the sample in as-cast condition revealed presence of three phases: Cu₃Sn, Cu₆Sn₅ and Sn. The microstructure of the sample is shown in figure 1a, and identification of particular phases is presented in figure 1b. To quantify their percentage fraction on the sample, the digital image analysis had been performed, using NIS Elements software. The results are presented in table 2. It is visible, that the phases Cu₃Sn and Cu₆Sn₅ occupy almost the same area of the sample. Conducted analysis confirmed that measured chemical composition was in good agreement with nominal one.

Table 2. Percentage share of the area occupied by particular phases in as-cast condition.

	Cu ₃ Sn	Cu ₆ Sn ₅	Sn
Percentage share of phase, %	118.7	16.510	7.19

SEM analyses were also performed for samples after sedimentation process. The microscopic investigations were conducted on different areas of the samples to verify if there are any changes in phases morphology due to sedimentation process. Three different spots were chosen on the sample. First spot was located close the maximum radius of the apparatus (figure 2a), second in the middle of the sample (figure 2b) and third was situated close to the centre of rotation (figure 2c). For all the samples, brightest colour indicates Sn and the darkest presents Cu₃Sn phase.



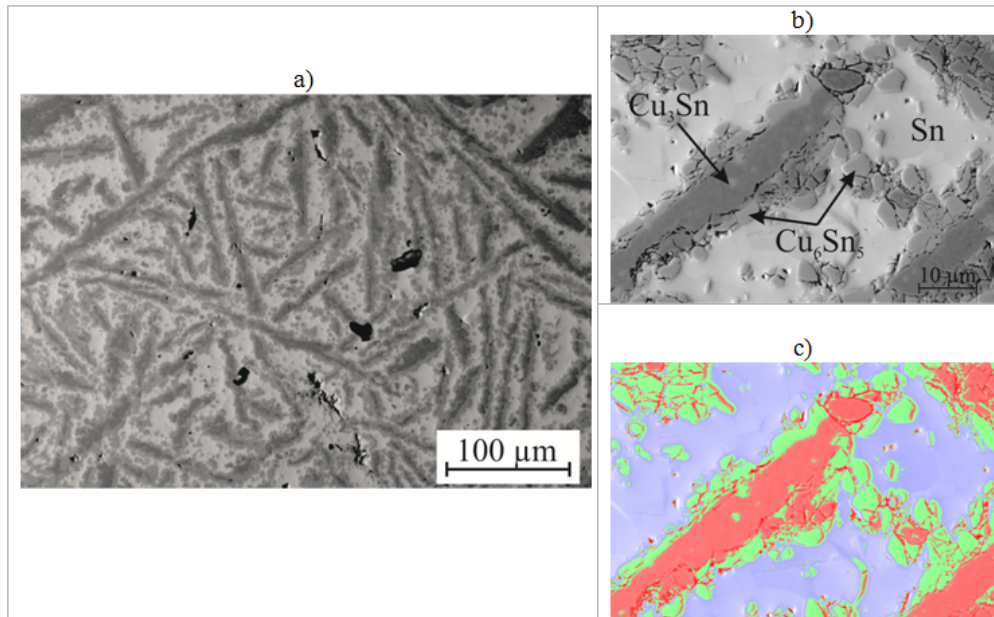


Fig. 1. Microstructures of Cu₃₀Sn₇₀ alloy in the as cast condition: (a) SEM microphotograph: magnification 270x, (b) SEM microphotograph: magnification 1900x – identification of particular phases is presented, (c) results of digital software analysis performed by NIS Elements Software – areas of occurrence of particular phases are depicted: red – Cu₃Sn, green – Cu₆Sn₅, grey – Sn.

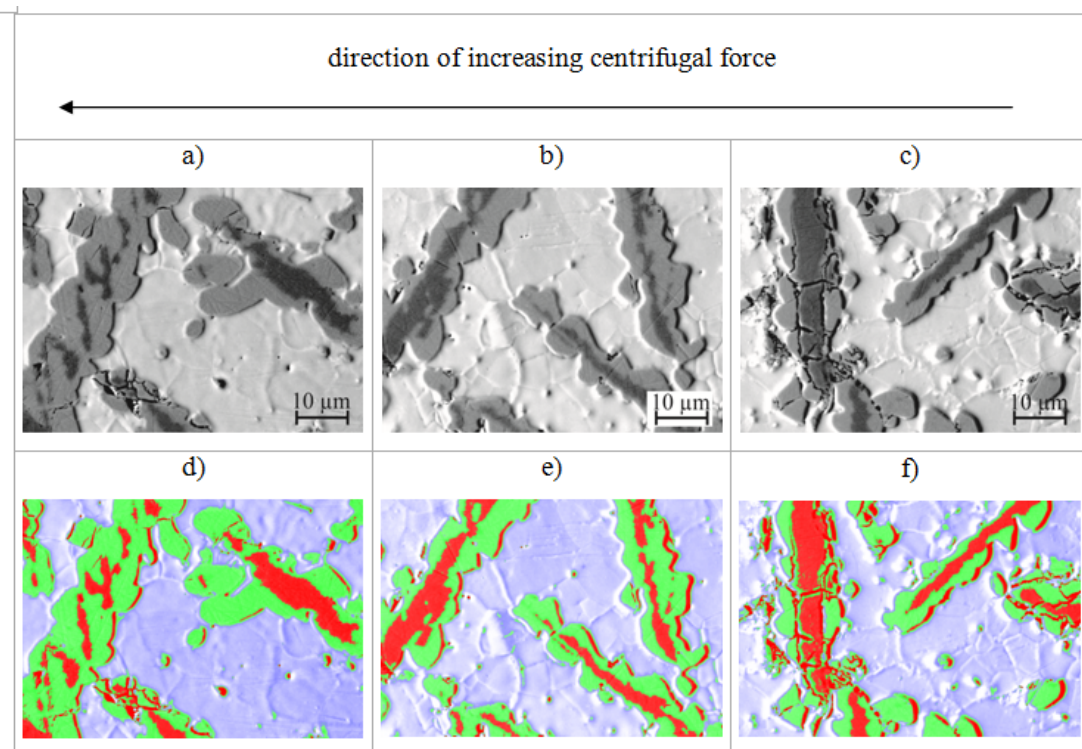


Fig. 2. SEM observations of Cu₃₀Sn₇₀ samples after sedimentation: (a-c) changes in microstructure, when centrifugal force increased, (d-f) examples of digital image analysis' results of the samples, where phases identification is shown: red – Cu₃Sn, green – Cu₆Sn₅

Table 3. Percentage fraction of the area occupied by particular phases in the samples after sedimentation. Number of sample is related to the order presented in figure 2

Number of sample	Cu ₃ Sn		Cu ₆ Sn ₅		Sn	
	Percentage fraction, %	Standard deviation	Percentage fraction, %	Standard deviation	Percentage fraction, %	Standard deviation
a)	8.82	0.93	26.57	2.56	64.61	1.70
b)	11.95	0.78	24.97	2.97	63.08	2.31
c)	16.89	1.60	23.92	1.18	59.18	1.33

Phase, that surrounds Cu₃Sn, has been identified as a Cu₆Sn₅. It is almost impossible to notice any changes in percentage share of Sn and Cu₆Sn₅ phases using unarmed eye, however, it is clearly visible that the area occupied by Cu₃Sn increased as the distance from the centre of rotation decreased. Results of digital image analysis (figure 2d-f) revealed that there are changes in percentage share of phases (table 3).

Comparing the data presented in table 2 and in table 3 it is clearly visible that percentage fraction of particular phases changed due to sedimentation process. The most vivid differences are observed for Cu₃Sn and Sn fractions. Increasing centrifugal force resulted in migration of heavier atoms of Sn (table 1) to the outer side of the sample and lighter atoms of Cu in the opposite direction. Thus, Cu₃Sn phase occupied almost two times greater area closer to the centre of rotation than on the maximum radius of ultracentrifuge apparatus. Such observations and conclusions are further explained and proved in mathematical modelling of sedimentation process in Cu₃₀Sn₇₀ alloy.

4. MODELLING

The Cu₃Sn and Cu₆Sn₅ phase growth. During the diffusion in Cu and Sn system, according to the phase diagram two intermetallic phases should grow at 453K, namely Cu₃Sn and Cu₆Sn₅. The growth of these phases in binary multiphase system can be calculated by the Leibnitz rule:

$$\frac{d}{dt} \int_{a(t)}^{b(t)} f(x,t) dx = \int_{a(t)}^{b(t)} \frac{\partial}{\partial t} f(x,t) dx + \dot{b}(t) f(t,b) - \dot{a}(t) f(t,a) \tag{1}$$

where: $f(x,t)$ - any continuous and differentiable function of position and time, $a(t)$, $b(t)$ - the positions of the boundaries which are moving with time:

$$\left(\dot{a}(t) = \frac{da(t)}{dt}, \dot{b}(t) = \frac{db(t)}{dt} \right)$$

The Leibnitz rule is the mass conservation law for moving boundary as presented in figure 3.

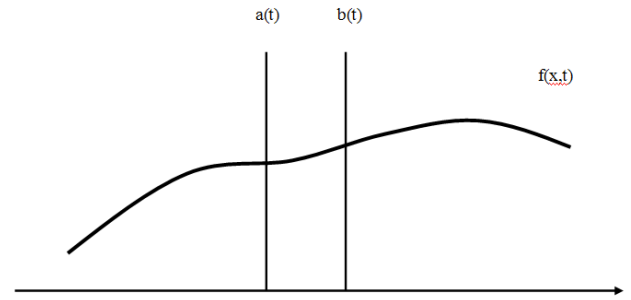


Fig. 3. The schematic presentation of Leibnitz rule.

In case of multiphase binary A-B diffusion couple in Leibnitz rule, the $f(x,t)$ function is concentration of the component, e.g. N_B . Moreover, the space between the boundaries at positions $a(t)$ and $b(t)$ is constant. Two phase zone (in the case of binary diffusion cannot be generated), thus:

$$\lim_{t \rightarrow \infty} b(t) - a(t) = const. \tag{2}$$

In consequence, the following equation can be written from the Leibnitz rule:

$$\frac{d}{dt} \int_{a(t)}^{b(t)} N_B(x,t) dx = \int_{a(t)}^{b(t)} \frac{\partial}{\partial t} N_B(x,t) dx + \dot{b}(t) N_B(t,b) - \dot{a}(t) N_B(t,a) \tag{3}$$

In this case the time differentials of the $a(t)$ and $b(t)$ are the fluxes of the B component at the left and right side of the phase boundary, e.g. the flux between Cu₃Sn and Cu₆Sn₅. Thus, the following expression can be written:

$$0 = \frac{d}{dt} \int_{a(t)}^{b(t)} N_B(x,t) dx = (N_B^{Cu_3Sn} - N_B^{Cu_6Sn_5}) \frac{dX^{Cu_3Sn/Cu_6Sn_5}}{dt} - j_B^{Cu_3Sn} + j_B^{Cu_6Sn_5} \tag{4}$$

where: N_B^k and j_B^k denote the concentration and the flux of the element B in the k -th phase, respectively and X^{Cu_3Sn/Cu_6Sn_5} is the position of the phase boundary between Cu₃Sn and Cu₆Sn₅ phase.

Following equation (4) the position of the phase boundary can be calculated:

$$\frac{dX^{Cu_3Sn/Cu_6Sn_5}}{dt} = \frac{j_B^{Cu_3Sn} - j_B^{Cu_6Sn_5}}{N_B^{Cu_3Sn} - N_B^{Cu_6Sn_5}} \tag{5}$$

Because of lack in the literature of kinetic data for Cu-Sn system at 453 K, interdiffusion coeffi-



cients have been taken as the same in value as the coefficients already used in calculations by Danielewski et al. (2011) for 473 K. In the calculations low nonstoichiometry that is low deviation from stoichiometric composition (ΔN_{Sn}) is also assumed. The interdiffusion coefficients and the data used in modelling of the phase growth in binary Cu-Sn system at 453 K are presented in table 4. Molar masses of the phases have been calculated based on the molar masses of pure components Cu and Sn at 500 K (table 1) and stoichiometry of particular phase (Cu_3Sn and Cu_6Sn_5).

Table 4. The data used in the modelling of the phase growth in binary Cu-Sn system (Danielewski et al., 2011).

Phase, j	Cu_3Sn	Cu_6Sn_5
ΔN_{Sn}	0.005	0.01
Interdiffusion coefficient, cm^2s^{-1}	1.1×10^{-11}	1.2×10^{-11}
Molar mass, $g \cdot mol^{-1}$	77.33	88.61

In figure 4, the kinetics of the phase growth in Cu-Sn alloy is shown. The Cu_3Sn phase grows slower than Cu_6Sn_5 . The values of the diffusion flux, such as interdiffusion coefficients multiplied by the gradient of the concentration in phase, confirm this observation. Moreover, the kinetic is parabolic, because the process is controlled by the diffusion.

Migration of pure Sn. In case of the sedimentation the additional process occurs - mainly the migration of the heavier component according to the centrifugal force acting. In case of the binary Cu-Sn system pure Sn is migrating outside the rotation centre. Thus, both phases Cu_3Sn and Cu_6Sn_5 migrate to the centre. Moreover, the Cu_3Sn fraction should be higher in the centre of the rotation and decrease with the centrifugal force - Cu_3Sn is lighter than Cu_6Sn_5 (table 4). The phase fraction of the phases can be calculated from the mass conservation law in a two-phase zone. The phase fractions of phases and are expressed as:

$$f_\alpha + f_\beta = 1 \quad (6)$$

Thus, the mass conservation law is:

$$\frac{\partial f_\alpha}{\partial t} = -\frac{\partial}{\partial x} (\Omega_\alpha J_\alpha) \quad (7)$$

where: Ω - constant volume of the α phase, J_α - the flux, expressed as:

$$\Omega_\alpha J_\alpha = \frac{f_\alpha D_\alpha}{kT} \left(F_\alpha^{ext} + \Omega_\alpha \frac{\partial \sigma}{\partial x} \right) + f_\alpha v^D \quad (8)$$

where: F_α^{ext} - the external force per unit mass of the i -th phase ($i = \alpha, \beta$).

Drift velocity v^D is given after Darken expression as follows:

$$v^D = -\frac{f_\alpha D_\alpha F_\alpha^{ext} + f_\beta D_\beta F_\beta^{ext}}{kT} - \frac{f_\alpha D_\alpha \Omega_\alpha + f_\beta D_\beta \Omega_\beta}{kT} \frac{\partial \sigma}{\partial x} \quad (9)$$

Combining equations (9) and (8) and (7), the following final expression can be written:

$$\frac{\partial f_\alpha}{\partial t} = \frac{\partial}{\partial x} \left[(f_\alpha f_\beta) \left(\frac{D_\beta F_\beta^{ext} - D_\alpha F_\alpha^{ext}}{kT} + \frac{D_\beta \Omega_\beta - D_\alpha \Omega_\alpha}{kT} \frac{\partial \sigma}{\partial x} \right) \right] \quad (10)$$

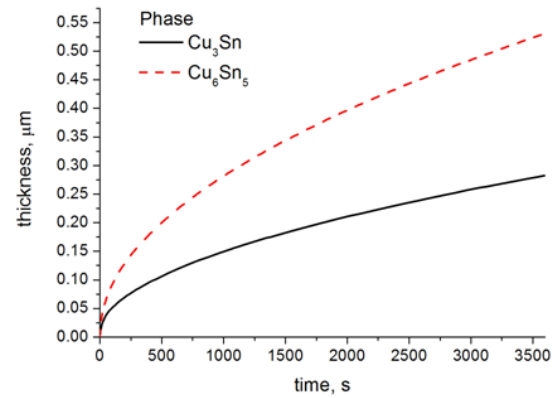


Fig. 4. Kinetics of growth of Cu_3Sn and Cu_6Sn_5 phases during diffusion process at 453 K.

In case of centrifugal force the F_β^{ext} can be calculated from stationary version of equation of motion as:

$$F_\alpha^{ext} = m_\alpha g = m_\alpha \omega^2 R \quad (11)$$

where: m_α - the mass of the elements of α phase, ω , R - the angular speed and radius of the system, respectively.

The stress can be calculated directly from the Darken velocity (Wierzbna, 2012) as follows:

$$\frac{\partial \sigma}{\partial t} = -\frac{E}{3(1-2\nu)} \frac{\partial v^D}{\partial x} \quad (12)$$

where: E - the Young modulus, ν - the Poisson ratio.



The calculations are performed for Cu_3Sn . The masses of the phases and data used in simulations are presented in table 4.

In case of the sedimentation process in the two-phase zone, the phases move from one part of the sample into the second one. Thus, the heavier phase is migrating according to the centrifugal force direction. The Cu_3Sn phase migrates into the centre of the sample. In figure 5 the normalised phase fraction profile is presented. From figure 5 one can conclude that the centrifugal force causes the Cu_3Sn phase migration into the centre of the sample at 453 K after 1 hour of the process.

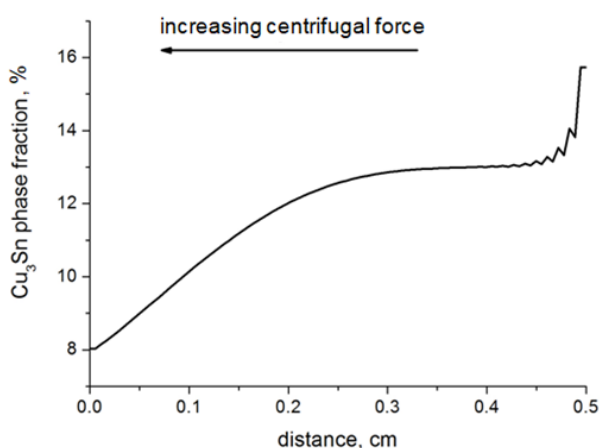


Fig. 5. The results of the sedimentation process - the normalized phase fraction profile.

5. CONCLUSIONS

To study the influence of sedimentation process on Cu_3Sn alloy, some experiments and mathematical modelling were performed. They resulted in formulating the following conclusions:

1. In as-cast condition in Cu_3Sn alloy, three different phases are visible, such as Cu_3Sn , Cu_5Sn_6 and Sn.
2. Sedimentation process of Cu_3Sn results in differences in percentage fraction of particular phases. Sn moves along the direction of increasing centrifugal force and Cu_3Sn phase in the opposite way.
3. Sedimentation process in Cu_3Sn can be successfully simulated by Leibnitz rule – results of percentage fraction of particular phases obtained after experiment were in good agreement with calculations.

ACKNOWLEDGMENTS

This work has been supported by the National Science Centre (NCN) in Poland, decision number 2015/19/B/ST8/00999.

REFERENCES

- Anthony, T.R., 1970, Sedimentation in the solid state, *Acta Metall.*, 18, 877-880.
- Barr, L.W., Smith, F.A., 1969, Observations on the equilibrium distribution of gold diffusing in solid potassium in a centrifugal field, *Phil. Mag.*, 20, 1293-1294.
- Danielewski, M., Wierzba, B., Gusak, A., Pawekiewicz, M., Janczak-Rusch, J., 2011, Chemical interdiffusion in binary systems; interface barriers and phase competition, *J. Appl. Phys.* 110, 123705.
- Demeler, B., Saber, H., 1998, Determination of molecular parameters by fitting sedimentation data to finite-element solutions of the Lamm equation, *Biophys. J.*, 74, 1, 444-454.
- Haynes, W. M. 2009. *CRC handbook of chemistry and physics: a ready-reference book of chemical and physical data*, Boca Raton: CRC Press.
- Huang, X., Mashimo, T., Ono, M., Tomita, T., Sawai, T., Osakabe, T., Mori, N., 2004. Effects of ultrastrong gravitational field on the crystalline state of a Bi-Sb alloy, *J. Appl. Phys.*, 96, 1336-1340.
- Lamm, O., 1929, Die Differentialgleichung der Ultrazentrifugierung, *Ark. Mat. Astron. Fys.*, 21B, 1-4.
- Mashimo, T., 1988, Self-consistent approach to the diffusion induced by a centrifugal field in condensed matter: Sedimentation, *Phys. Rev. A.*, 38, 8, 4149-4154.
- Mashimo, T., Okazaki, S., Shibasaki, S., 1996, Ultracentrifuge apparatus to generate a strong acceleration field over 1000000 g at a high temperature in condensed matter, *Rev. Sci. Instrum.*, 67, 9, 3170-3197.
- Mashimo, T., Ono, M., Huang, X.S., Iguchi, Y., Okayasu, S., Kobayashi, K., Nakamura, E., 2008, Gravity-induced diffusion of isotope atoms in monoatomic solid Se, *EPL*, 81, 56002.
- Ono, M., Sueyoshi, M., Okayasu, S., Esaka, F., Osawa, T., Iguchi, Y., Mashimo, T., 2009, Development of special rotor for centrifugal separation of isotopes in solid pure metals, *Rev. Sci. Instrum.* 80, 8, 083908.
- Wierzba, B., 2012, Entropy production in Cu-Fe-Ni alloys - The bi-velocity method, *Physica A*, 391, 56-61.
- Wierzba, B., 2017, The vacancies formation and agglomeration under centrifugal force, *Physica A*, 484, 482-487.
- Wierzba, B., Mashimo, T., Danielewski, M., 2018, Competition between chemical and gravity forces in binary alloys, *High Temp. Mater. Proc.*, 37, 285-288.
- Wierzba, B., Nowak, W.J., 2018, The Changes in the morphology of Bi-Sb system under centrifugal force at room temperature, *Materials*, 11, 1065-1071.



**SEDYMENTACJA W DWUSKŁADNIKOWYM
UKŁADZIE Cu-Sn****Streszczenie**

W niniejszej pracy zaprezentowano proces sedymentacji w dwuskładnikowym, wielofazowym układzie Cu-Sn. Do eksperymentów zastosowano próbki wyprodukowane przez GoodFellow o początkowym składzie molowym Cu₃₀Sn₇₀, co implikuje otrzymanie obszaru dwufazowego. W eksperymencie obserwowane są dwa zjawiska – wzrost faz Cu₃Sn oraz Cu₆Sn₅ – na skutek wzrostu temperatury oraz migracja atomów czystej cyny pod wpływem działającej siły odśrodkowej. Oba zjawiska mogą zostać opisane równaniami fizycznymi. Model opisujący wzrost faz bazuje na zasadzie Leibniza. Prawo zachowania masy na przesuwałej się granicy i migracja pierwiastków na skutek sedymentacji scharakteryzowane są równaniem ruchu. W pracy zawarto wyniki badań eksperymentalnych oraz wyniki obliczeń sprawdzających poprawność przedstawionych modeli matematycznych.

Received: October 15, 2018.

Received in a revised form: November 3, 2018.

Accepted: December 21, 2018.

